TSINGHUA SCIENCE AND TECHNOLOGY
ISSN 1007-0214 12/14 pp127–139
DOI: 10.26599/TST.2018.9010143
Volume 25, Number 1, February 2020

Collision Avoidance Strategy Supported by LTE-V-Based Vehicle Automation and Communication Systems for Car Following

Jiayang Li, Yi Zhang*, Mengkai Shi, Qi Liu, and Yi Chen

Abstract: We analyzed and improved a collision avoidance strategy, which was supported by Long Term Evolution-Vehicle (LTE-V)-based Vehicle-to-Vehicle (V2V) communication, for automated vehicles. This work was completed in two steps. In the first step, we analyzed the probability distribution of message transmission time, which was conditional on transmission distance and vehicle density. Our analysis revealed that transmission time exhibited a near-linear increase with distance and density. We also quantified the trade-off between high/low resource reselection probabilities to improve the setting of media access parameters. In the second step, we studied the required safety distance in accordance with the response time, i.e., the transmission time, derived on the basis of a novel concept of Responsibility-Sensitive Safety (RSS). We improved the strategy by considering the uncertainty of response time and its dependence on vehicle distance and density. We performed theoretical analysis and numerical testing to illustrate the effectiveness of the improved robust RSS strategy. Our results enhance the practicability of building driverless highways with special lanes reserved for the exclusive use of LTE-V vehicles.

Key words: vehicle automation and communication; collision avoidance; Long Term Evolution-Vehicle (LTE-V); Responsibility-Sensitive Safety (RSS)

1 Introduction

During the last decade, the government, research institutions, and the automobile industry have contributed enormous interdisciplinary effort to the development, testing, and employment of Vehicle Automation and Communication Systems (VACS) to improve road safety[1]. Collision avoidance is an indispensable expected application of VACS[2]. A reliable sensing system is necessary for understanding the present state of the environment, including the position and speed of surrounding vehicles, to prevent collision.

Vehicle-to-Vehicle (V2V) communication, one of the most promising vehicular technologies, can serve as a sensing system. Various wireless access technologies, including Wi-Fi, Dedicated Short Range Communication (DSRC), Long Term Evolution-Vehicle (LTE-V), and infrared communications, are used for V2V communication. LTE-V is currently utilized to support vehicular applications because of its high reliability, large bandwidth[3], global deployment, and rapid commercialization[4]. The initial standards supporting V2V services were established in 2016 and

• Jiayang Li is with the Department of Mathematics, Tsinghua University, Beijing 100084, China. E-mail: jy-li15@ mails.tsinghua.edu.cn.
• Yi Zhang is with Beijing National Research Center for Information Science and Technology (BNRist), Department of Automation, Tsinghua University, Beijing 100084, China, and with Tsinghua-Berkeley Shenzhen Institute (TBSI), Shenzhen 518055, China, and also with Jiangsu Province Collaborative Innovation Center of Modern Urban Traffic Technologies, Nanjing 210096, China. E-mail: zhyi@tsinghua.edu.cn.
• Mengkai Shi is with Beijing Nebula Link Tech. Co. Ltd, Beijing 100080, China. E-mail: smk@nabula-link.com.
• Qi Liu and Yi Chen are with Network Technology Research Institute, China Unicom, Beijing 100044, China. E-mail: {liuqi49, cheny1086}@chinaunicom.cn.
∗ To whom correspondence should be addressed.
Manuscript received: 2018-09-13; revised: 2018-12-04; accepted: 2018-12-11

@ The author(s) 2020. The articles published in this open access journal are distributed under the terms of the Creative Commons Attribution 4.0 International License (http://creativecommons.org/licenses/by/4.0/).

further enhanced in 2017. Additional details regarding the standards can be found in the original technical report published by 3GPP[5–11] and summarized in recent papers[3, 4, 12].

V2V communication technologies promise to improve safety drastically by reducing the delay in emergency message propagation. For example, the leading vehicle can send warning messages when abruptly decelerating[13]. If the following vehicle can receive the message with minimal delay, then it can decelerate automatically to prevent collision. Automated vehicles must maintain a safe distance in advance to improve the chance of collision avoidance[14]. The required safety distance is positively correlated with response time. Thus, safety distance is also correlated with the delay of message transmission.

Different strategies for the derivatization of the required safety distance have been designed. The research group of Mobileye recently proposed the novel concept of Responsibility-Sensitive Safety (RSS) for the derivatization of safety distance under the assumption of constant response time[14]. RSS attempts to establish a formal foundation that sets all aspects of human judgment in the context of driving with the goal of setting a formal standard of safety for autonomous vehicles[15]. This concept promises that if a self-driving car drives responsibly, it will never cause an accident even if it might still become involved in an accident[16, 17]. In this strategy, vehicles adopt a situation-unaware strategy that results in an unnecessarily large gap between vehicles. However, human drivers maintain small gaps between vehicles in numerous practical situations[18, 19]. Therefore, a previous work proposed an improved strategy[20] wherein the vehicle is aware of its state. The proposed strategy improved the balance between traffic safety and efficiency.

In the present work, we evaluated the RSS strategy for collision avoidance supported by V2V technology in two steps. The first step involves the evaluation of the LTE-V-based V2V message transmission time. We proposed a Markov model to describe the Media Access Control (MAC) process of LTE-V. Then, we derived the probability distribution of transmission time for different MAC parameter settings. Transmission time is conditional on transmission distance, node density, and radio range. The second step involves the analysis of the RSS strategy supported by V2V communication. In the collision avoidance system, the warning message transmission time is simply the response time of RSS, which bridges the two steps. The analysis of RSS strategy in this work is more thorough than that in previous studies. First, given that transmission distance can be acquired from the vehicle communication system, we further extended the situation-aware strategy by incorporating information. Second, given that response time is regarded as a random variable instead of constant[14, 20], we improved the robustness of safety by overcoming uncertainty. We provided suggestions for different scenarios on the basis of performance analysis.

We organized the rest of the paper as follows to present our findings effectively: Section 2 provides an analysis of the MAC process of LTE-V. Then, the derivatization of the probability distribution of V2V message transmission time under different circumstances is discussed in Section 3. The original and improved RSS strategy is provided in Section 4. An analysis of the performance of LTE-V-based RSS for car following is also given in this section. Finally, the conclusion is presented in Section 5.

2 Modeling of the MAC Process

We analyzed Release 14 of LTE-V for the support of direct V2V communications. This release was completed in 2017 and includes two modes: modes 3 (LTE-V-Cell) and 4 (LTE-V-Direct), as shown in Fig. 1. The two modes are differentiated on the basis of their allocation of radio resources. Mode 3 requires cellular coverage, whereas mode 4 uses a distributed scheduling scheme. Mode 4 is considered as the baseline mode and represents an alternative to DSRC[12]. In this work, we focus solely on mode 4. The nomenclatures related to LTE-V-Direct are given in Table 1, which can be used as a reference in the following sections.

2.1 MAC protocol

LTE-V-Direct is the standard for high-speed wireless communication based on the Time-Division Multiple Access (TDMA) protocol. TDMA allows users to share the same frequency channel by dividing a signal into

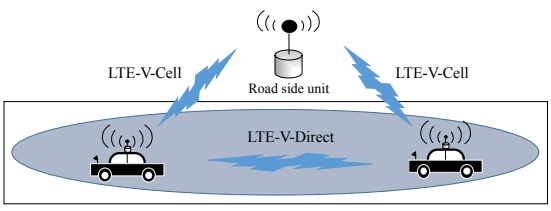

Fig. 1 Two kinds of LTE-V modes.

Table 1 Nomenclature list of LTE-V-Direct.

Symbol	Definition
t_{frame}	Time of a frame (resource reservation period)
n_{slot}	Number of slots in a frame
T_{counter}	State of the resource reselection counter
p_{rr}	Resource reselection probability
T_{rr}	Resource reselection interval
$\{X_n\}$	Backward transmission state number
$\{Y_n\}$	Forward transmission state number
$\{\pi_i\}$	Stationary probabilities of state number
ρ_{lag}	Transmission time lag of LTE-V
p_{rupt}	Transmission interruption probability
T_{rec}	Transmission recovery time
R	Radio range of LTE-V
λ	Average node density

frames (resource reservation period) and a frame into time slots (channel). Users transmit in rapid succession by using its own time slot in every frame. Therefore, the MAC protocol is necessary for efficient resource allocation. The MAC process of LTE-V-Direct[5–11] can be summarized as follows and the corresponding flowchart is shown in Fig. 2:

(1) The node checks the slot occupied information of the previous one frame (or several frames) and randomly selects one idle slot. It records $Slot = i$ if it is the i-th slot.

(2) The node randomly selects an integer j from 5 to 15. It records $T_{\text{counter}} = j$.

(3) The node uses the slot recorded in *Slot* to transmit during the next T_{counter} frames.

(4) The node conducts a Bernoulli trial with the expectation p_{rr}: go back to Step 1 if the outcome is 1 and return to Step 2 otherwise.

Resource selection is based on channel listening information. Nodes, however, cannot use one channel forever. Transmission collision is unavoidable given the dynamic topology of vehicles and other reasons. Therefore, resource reselection is necessary to terminate simultaneous transmissions. In this work, we defined the interval between resource reselection as the resource reselection interval T_{rr}. The performance of the LTE-V protocol mainly depends on the distribution of T_{rr}. However, a trade-off when scheduling T_{rr} exists:

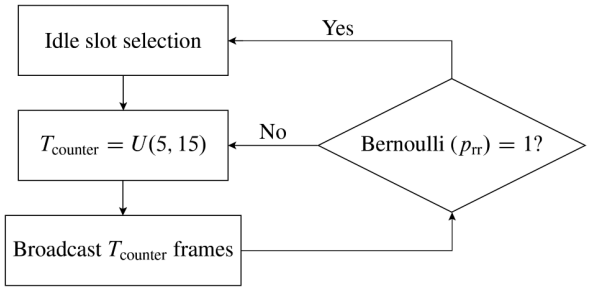

Fig. 2 Flowchart of the original protocol.

• The probability of transmission collision is positively correlated with the expectation of T_{rr}. Vehicles will fail to acquire each other's latest slot information if they change channels simultaneously. Therefore, the resource reselection intervals for different vehicles are requested to be sufficiently stochastic. Accordingly, a large variation in T_{rr} is required. This requirement results in a large T_{rr}.

• The duration of transmission collision is negatively correlated with the expectation of T_{rr}. Nodes need to change to a new channel promptly on the basis of the latest listening information to terminate possible transmission collision resulting from concurrent slot occupation. Therefore, to achieve this goal, T_{rr} is requested to be as small as possible.

We need to model T_{rr} to analyze the performance of LTE-V-Direct from these two aspects. The following two state parameters are proposed for the analysis of T_{rr}:

• Backward transmission state number $\{X_n\}$. Let $X_n = m$ denote that the node will use the current slot for m frames (including the current frame) during the n-th frame.

• Forward transmission state number $\{Y_n\}$. Let $Y_n = m$ denote that the node has used the current slot for m frames (including the current frame) during the n-th frame.

2.2 Transmission state number

Under the original MAC protocol, the backward transmission state number of a node during a frame is determined by its value during the last frame and whether it will continue using this slot when T_{counter} decreases to 0, a state that is difficult to analyze. As shown in Fig. 2, conducting the Bernoulli trial in Step 4 after Step 3 is unnecessary. The node can initiate Step 4 immediately after Step 2 and add up T_{counter} until the Bernoulli trial provides a value of 0. Thus, the procedure can be modified without changing the actual effects. The modified procedure can be summarized as follows and the corresponding flowchart is shown in Fig. 3.

(1) The node checks the slot-occupied information of the previous frame and randomly selects one slot from

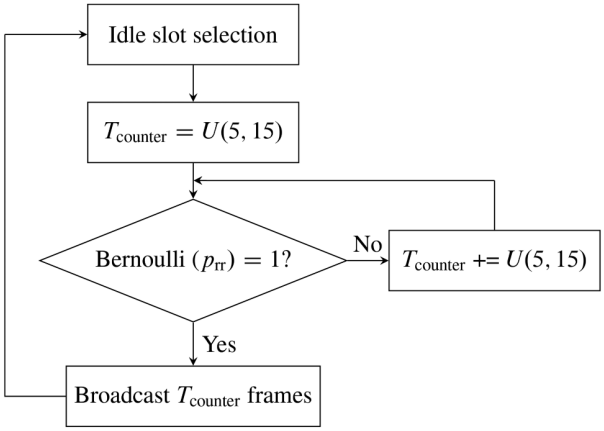

Fig. 3 Flowchart of the modified protocol.

idle slots. It records $Slot = i$ if it is the i-th slot.

(2) The node randomly selects an integer j from 5 to 15. It records $T_{\text{counter}} = j$.

(3) The node conducts a Bernoulli trial with the expectation p_{rr}. If the outcome is 1, it goes back to Step 4. If the outcome is 0, it randomly selects an integer j from 5 to 15, records $T_{\text{counter}} = T_{\text{counter}} + j$ and then returns to Step 3.

(4) The node uses the slot recorded in *Slot* to transmit during the next T_{counter} frames.

As shown in the above modification, the backward transmission state number of the node is determined only by its value in the last frame. Accordingly, it becomes a Markov chain that can be analyzed. It is a stochastic process that takes on all positive integers. Let K denote the number of times Step 2 occurs in a cycle. Then, K follows geometric distribution, and the probability that K takes a large value can be ignored. Therefore, $K \leqslant k_{\max}$, i.e., $T \leqslant 15k_{\max}$, can be assumed. In this work, we set $k_{\max}$ as 30. The probability that $K \leqslant k_{\max}$ is represented as follows:

$$p_{\text{sum}} = \sum_{k=1}^{k_{\max}} (1 - p_{\text{rr}})^{k-1} p_{\text{rr}} \tag{1}$$

Under this assumption, only two kinds of transitions are involved as shown below:

$$\begin{cases} P(X_{n+1} = i - 1 | X_n = i), & 2 \leqslant i \leqslant 15k_{\max}, \\ P(X_{n+1} = j | X_n = 1), & 5 \leqslant j \leqslant 15k_{\max}. \end{cases}$$

Whenever the process is in state i, there is a fixed probability exists that it will next be in state j. Thus, we can denote $P(X_{n+1} = j | X_n = i)$ as $P_{i,j}$. Given that when $2 \leqslant i \leqslant 15k_{\max}$, $P_{i,i-1} = 1$, we only need to compute $P_{1,j}$. For a particular j, we have $j/15 + 1 \leqslant K \leqslant j/5$, thus we can derive that $P_{1,j}$ equals

$$\sum_{k=j/15+1}^{j/5} P(X_{n+1} = j | X_n = 1, K = k) \times P(K = k | K \leqslant k_{\max}) \tag{2}$$

Given that K obeys a geometric distribution, $P(K = k | K \leqslant k_{\max}) = (1 - p_{\text{rr}})^{k-1} p_{\text{rr}} / p_{\text{sum}}$. Meanwhile, we can obtain that

$$P(X_{n+1} = j | X_n = 1, K = k) = \frac{1}{11^k} \text{choice}(j, k) \tag{3}$$

where choice(j, k) is the number selected to divide a queue of j into k portions with lengths between 5 and 15. There are up to $a = (j - 5m)/11$ portions that have at least 16 elements. Thus, choice(j, k) equals the number chosen to divide a queue of j into k portions of at least 5, minus 1 portion of at least 16 while $k - 1$ portions of at least 5, plus 2 portions of at least 16 while $k - 2$ portions of at least 5, until minus/plus a portions of at least 16 while $k - a$ portions of at least 5. In conclusion,

$$\text{choice}(j, k) = \mathbf{C}_{j-4k-1}^{k-1} + \sum_{l=1}^{(j-5m)/11} (-1)^i \mathbf{C}_{j-15l-4(k-l)-1}^{k-1} \mathbf{C}_k^l \tag{4}$$

Eventually, we have

$$P_{1,j} = \sum_{k=j/15+1}^{j/5} \frac{1}{11^k} \text{choice}(j, k) \frac{(1 - p_{\text{rr}})^{k-1} p_{\text{rr}}}{p_{\text{sum}}} \tag{5}$$

We denote $\{\pi_i\}_{i=1}^{15k_{\max}}$ as the stationary probabilities of states. Then, given that the Markov chain is positive recurrent, the stationary probabilities can be obtained by solving the following equations:

$$\begin{cases} \pi_j = \sum\limits_j \pi_i P_{i,j}, \\ \sum\limits_j \pi_j = 1 \end{cases} \tag{6}$$

The solution is

$$\begin{cases} \pi_1 = \dfrac{1}{1 + \left(\sum\limits_{l_1=2}^{15k_{\max}} \left(1 - \sum\limits_{l_2=1}^{l_1-1} P_{1,l_2} \right) \right)}, \\ \pi_i = \pi_1 (1 - \sum\limits_{l=1}^{i-1} P_{1,l}), \ 2 \leqslant i \leqslant 15k_{\max} \end{cases} \tag{7}$$

where we assume that $P_{1,i} = 0$, $i = 2, 3, 4$.

The forward transmission state number during one frame is determined by both its value during the last frame and T_{counter} it selected at the beginning of this cycle. Thus, $\{Y_n\}$ is not a Markov chain. However, given that it can be regarded as the backward chain of $\{X_n\}$, the stationary probabilities of the two chains are

equal. We denote $\{\pi_i\}$ as the stationary probabilities of both $\{X_n\}$ and $\{Y_n\}$ as described in Section 3.

3 Modeling of the Transmission Time

This section presents an analysis of the V2V message transmission time ρ_{trans}. First, we need to decompose the transmission time in accordance with the collision avoidance process of VACS as illustrated in Fig. 4, where t_{pre} is the time for the leading vehicle to prepare for transmission, t_{react} is the time for the following vehicle to react after receiving the message, and ρ_{lag} is the transmission lag due to transmission collision. As shown in the flowchart, we have

$$\rho_{\text{trans}} = t_{\text{pre}} + \rho_{\text{lag}} + t_{\text{react}} \tag{8}$$

Here, t_{pre} includes the time preparing for the delivered message and the time waiting for its allocated channel in the next frame. We set $t_{\text{pre}} = 2t_{\text{frame}}$ on the basis of a conservative estimate. Meanwhile, we can set $t_{\text{react}} = t_{\text{frame}}$ because the vehicle receives the states of surrounding vehicles every frame. t_{pre} and t_{react} can be set as other values in accordance with real situations. We only need to analyze ρ_{lag}, and two questions need to be solved in advance, as follows: (1) whether the communication between the two vehicles is interrupted during the emergency, and (2) if so, the time required for the transmission to recover from the interruption.

We need to compute the probability of transmission interruption $p_{\text{rupt}} = P\{\rho_{\text{lag}} \neq 0\}$ to answer the first question. We need to compute the probability density function of transmission recovery time $f_{T_{\text{rec}}}(t) = P\{T_{\text{rec}} \leqslant t\}$ to answer the second question. T_{rec} is irrelevant to traffic flow, whereas vehicle density and transmission distance will affect p_{rupt}. We first analyzed

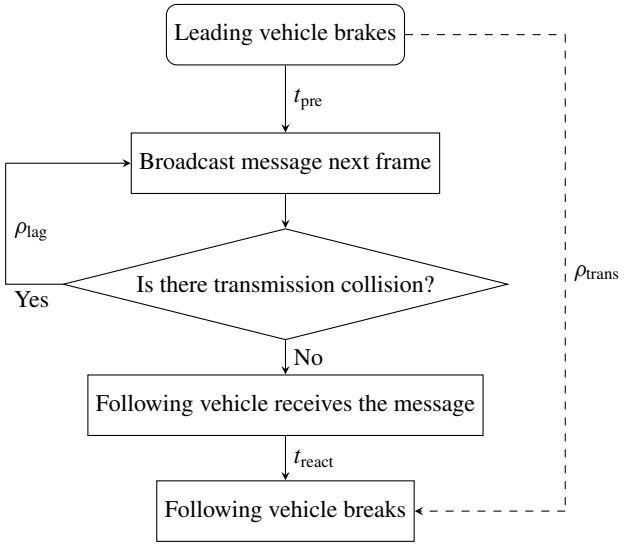

Fig. 4 Flowchart of collision avoidance process.

T_{rec}, and then derived p_{rupt} under different conditions.

3.1 Transmission recovery time

The radio range of Vehicle $\mathcal{V}$ is denoted as $Hop_{\mathcal{V}}$. If Vehicle $\mathcal{A}$ and Vehicle $\mathcal{B}$ are experiencing communication interruption, the backward state numbers of the two vehicles that occupy the same slot within $Hop_{\mathcal{B}}$ are i and j with probabilities π_i and π_j, respectively. Then, communication will resume after $i \wedge j$ frames when one vehicle changes channels. Therefore, we have

$$P\{T_{\text{rec}} = k t_{\text{frame}}\} = \pi_k(\pi_k + 2\sum_{i=k+1}^{15k_{\max}} \pi_i) \tag{9}$$

Then the cumulative distribution function of T_{rec} can be derived: for $t \in [k t_{\text{frame}}, (k+1)t_{\text{frame}}]$, we have

$$f_{T_{\text{rec}}}(t) = P\{T_{\text{rec}} \leqslant t\} = \sum_{j=1}^{k} \pi_j(\pi_j + 2\sum_{i=j+1}^{15k_{\max}} \pi_i) \tag{10}$$

Based on Eq. (10), the graph of $f_{T_{\text{rec}}}(t)$ is displayed in Fig. 5. As mentioned in Section 2.1, when p_{rr} is low, T_{rec} is high. This situation is undesirable.

3.2 Frame information loss rate

We first need to analyze the reason for transmission collision to derive p_{rupt}. Transmission collision is unavoidable if two vehicles within radio range of each other fail to acquire each other's latest frame information. We denote this probability as frame information loss rate p_{loss}. The computation of this rate is presented in this subsection. If Vehicle $\mathcal{A}$ decides to change slots at the i-th frame, then $\mathcal{A}$ will begin to use the new slot from the $(i+1)$-th frame. However, this slot is selected on the basis of the frame information acquired at the $(i-1)$-th slot. Accordingly, if another Vehicle $\mathcal{B}$ decides to change slots at the $(i-1)$-th, i-th, or $(i+1)$-th frame, frame information loss between Vehicle $\mathcal{A}$ and $\mathcal{B}$ will occur. Therefore, the

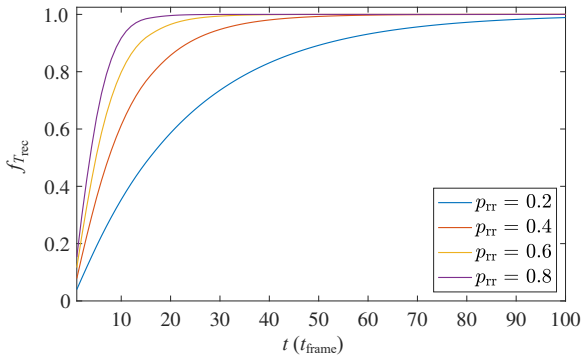

Fig. 5 Cumulative distribution function of T_{rec}.

sufficient and necessary condition for the loss of frame information is as follows: the forward transmission state number of $\mathcal{A}$ and $\mathcal{B}$ differs by at most 1, i.e., $|Y_n^{\mathcal{A}} - Y_n^{\mathcal{B}}| \leqslant 1$. Under this condition, when $\mathcal{A}$ is with $Y_n^{\mathcal{A}} = i$ (the probability is π_i), $\mathcal{B}$ needs to satisfy $Y_n^{\mathcal{B}} \in \{i-1, i, i+1\}$ (the probability is $\pi_{i-1} + \pi_i + \pi_{i+1}$). Therefore, we have

$$p_{\text{loss}} = \sum_{i=1}^{15k_{\max}} \pi_i(\pi_{i-1} + \pi_i + \pi_{i+1}) \tag{11}$$

where we assume that $\pi_0 = 0$ and $\pi_{15k_{\max}+1} = 0$.

The frame information loss rate for every p_{rr} can be computed by combining Eq. (11) with Eq. (7). The result is shown in Fig. 6.

3.3 Coupling of areas

In this model, we assume that no energy is detected from transmission beyond radio range R. Vehicle $\mathcal{B}$ in $Hop_{\mathcal{A}}$ can receive the packet broadcasted by Vehicle $\mathcal{A}$ if no vehicle in $Hop_{\mathcal{B}}$ occupies the same slot occupied by Vehicle $\mathcal{A}$. Therefore, we need to analyze the slot allocation of vehicles in $Hop_{\mathcal{B}}$, which can be divided into two subsets:

- One-hop collision area: $F = Hop_{\mathcal{B}} \cap Hop_{\mathcal{A}}$. Vehicles in this area and $\mathcal{A}$ share their frame information together. Thus F is a collision-free area. However, one-hop collision occurs when nodes change slots simultaneously.
- Hidden-terminal collision area: $H = Hop_{\mathcal{B}} \backslash Hop_{\mathcal{A}}$.

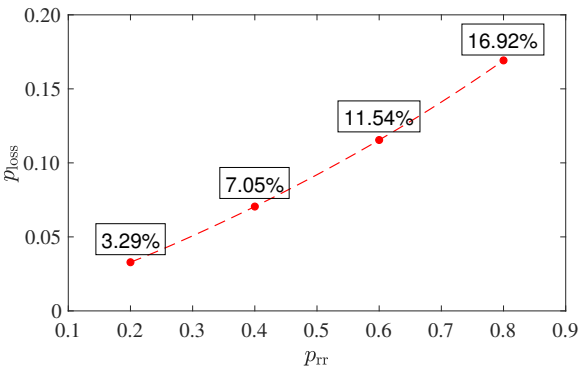

Fig. 6 Frame information loss rate.

Vehicles in this area lack the frame information of $\mathcal{A}$. Thus the slot occupied by $\mathcal{A}$ can be assigned to vehicles in this area. The erroneous assignment of occupied slots results in hidden-terminal collision.

The area division is presented in Fig. 7. For simplicity, if S is an area, we denote the event that no vehicle in S occupies the same slot of $\mathcal{A}$ in Area S as S and the mutually exclusive event of S as $!S$. Meanwhile, considering an event D, we abbreviate $P\{D\}$ as D.

The expected number of vehicles in $Hop_{\mathcal{B}}$ always remains constant no matter the distance d between $\mathcal{A}$ and $\mathcal{B}$. However, the lengths of F and H are $2R - d$ and d, respectively. Given that F is safer than H, p_{rupt} increases with d.

Then, we analyze the relationship between p_{rupt} and d. We denote $P = 1 - p_{\text{rupt}}$, i.e., the probability of successful transmission. Unfortunately, P cannot be expressed as $F \cdot H$ because event F and H are not independent. For example, if a vehicle $\mathcal{C}$ in F already occupies the same slot of $\mathcal{A}$, then $Hop_{\mathcal{A}} \cap Hop_{\mathcal{C}}$ will become a collision-free area. Instead, we have

$$P = F \cdot H|F \tag{12}$$

We need to consider the conditional probability of F and H to compute F,

$$\begin{cases} F = H \cdot F|H + !H \cdot F|!H, \\ H = F \cdot H|F + !F \cdot H|!F \end{cases} \tag{13}$$

We can then interpret F and H with conditional probabilities by regarding F and H as unknowns:

$$F = \frac{-F|!H - F|H \cdot H|!F + F|!H \cdot H|!F}{-1 + F|H \cdot H|F - F|!H \cdot H|F - F|H \cdot H|!F + F|!H \cdot H|!F} \tag{14}$$

Event H and E also depend on each other. When vehicle density is high, probability $!E$ is extremely high. Although vehicles in area E are out of $Hop_{\mathcal{B}}$, if a vehicle in E occupies the same slot as $\mathcal{A}$, it will reduce the probabilities $!F$ and $!H$. Thus, we also need to analyze the coupling of E and $F|H$, and the coupling of E and $F|!H$. We denote $F|H$ as F_1 and $F|!H$ as F_2. Similarly, we have

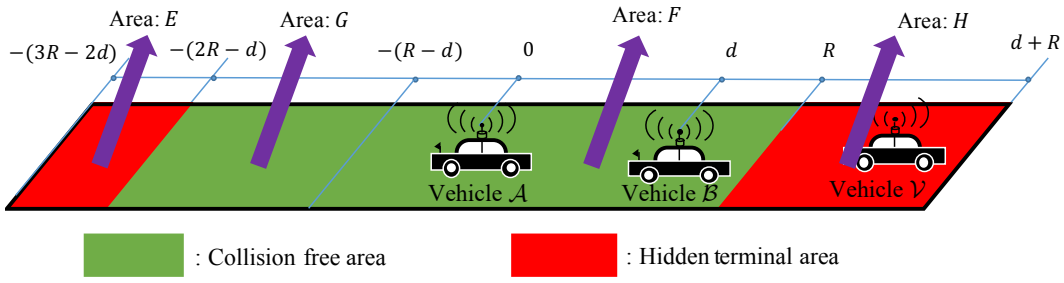

Fig. 7 Area division.

$$F_1 = \frac{-F_1|!E-F_1|E\cdot E|!F_1+F_1|!E\cdot E|!F_1}{-1+F_1|E\cdot E|F_1-F_1|!E\cdot E|F_1-F_1|E\cdot H|!F_1+F_1|!E\cdot E|!F_1} \tag{15}$$

$$F_2 = \frac{-F_2|!E-F_1|E\cdot E|!F_2+F_2|!E\cdot E|!F_2}{-1+F_2|E\cdot E|F_2-F_2|!E\cdot E|F_2-F_2|E\cdot H|!F_2+F_2|!E\cdot E|!F_2} \tag{16}$$

Eventually, we combine Eqs. (12), (14) – (16), then P can be expressed by a set of conditional probabilities.

3.4 Conditional successful probability

As discussed in Section 3.3, to derive P, we first need to compute all the conditional probabilities in Eqs. (14) – (16). As shown in Fig. 7, $H|F$, $H|!F$, $E|F_1$, $E|!F_1$, $E|F_2$, and $E|!F_2$ are conditional probabilities of collision in hidden terminal areas, whereas $F_1|E$, $F_1|!E$, $F_2|E$, and $F_2|!E$ are conditional probabilities of collision in one-hop areas. In this section, we analyze the two kinds of probabilities separately. We only discuss how to compute $H|F$ and $F_1|E$, and other probabilities can be derived in a similar way.

We make the following assumptions to simplify the problem: (1) We assume that all vehicles are at the center when analyzing an area S because the center is the expected position of vehicles following Poisson arrival. (2) If two vehicles $\mathcal{V}_1$ and $\mathcal{V}_2$ already occupy one slot, we ignore the probability that another vehicle in $Hop_{\mathcal{V}_1} \cap Hop_{\mathcal{V}_2}$ will also occupy this slot because it is a second-order small amount.

3.4.1 Hidden-terminal collision probability

As discussed in this section, we derived the probability of hidden-terminal collision. We first analyze $H|F$. We denote the left boundary and right boundary of the hidden terminal area H as $L_{\text{left}} = R$ and $L_{\text{right}} = R+d$, respectively. Then the center of H is

$$L_{\text{center}} = 0.5(L_{\text{left}} + L_{\text{right}}) \tag{17}$$

If one vehicle occupies the same channel as $\mathcal{A}$, other vehicles are not likely to select this channel. Thus, channel allocation in H is a sampling process without replacement. We denote the expected number of vehicles in H as n_{car} and denote the expected number of vehicles in $Hop_{\mathcal{A}} \cap Hop_{\mathcal{V}}$, where $\mathcal{V}$ is in $Hop_{\mathcal{B}}$, as n_{cap}. Given that λ is the average node density, we can compute the expected number of vehicles by using

$$n_{\text{car}} = \lambda(L_{\text{right}} - L_{\text{left}}) \tag{18}$$

$$n_{\text{cap}} = \lambda(2R - L_{\text{center}}) \tag{19}$$

The channels occupied by vehicles in $Hop_{\mathcal{A}} \cap Hop_{\mathcal{V}}$ share frame information with both $\mathcal{A}$ and $\mathcal{V}$, if the frame information is not lost. Thus, the expected number of channels that cannot be selected by $\mathcal{V}$ is

$$n_{\text{occupied}} = (1 - p_{\text{loss}})n_{\text{cap}} \tag{20}$$

Eventually, the probability that no vehicle in F occupies the channel of $\mathcal{A}$ is

$$P_{\text{hidden}} = \frac{\mathbf{C}^{n_{\text{car}}}_{n_{\text{slot}}-1-n_{\text{occupied}}}}{\mathbf{C}^{n_{\text{car}}}_{n_{\text{slot}}-n_{\text{occupied}}}} \tag{21}$$

Equations (17) – (20) illustrate that Eq. (21) only depends on L_{right} and L_{left}. Thus, we can denote Eq. (21) as $P_{\text{hidden}}(L_{\text{left}}, L_{\text{right}})$.

Then we need to compute $H|!F$, $E|F_1$, $E|!F_1$, $E|F_2$, and $E|!F_2$. When computing $H|F$, the left boundary of the hidden terminal area is exactly the left boundary of H. However, when computing $E|F_1$, based on the assumption in this section, the problem vehicle is located at the center of F. Thus, some part in H also becomes the collision-free area and the left boundary of the new hidden terminal area is $R + 0.5d$. Therefore, we obtain $H|!F = P_{\text{hidden}}(R + 0.5d, R + d)$. $E|F_1$, $E|!F_1$, $E|F_2$, and $E|!F_2$ can be derived similarly and we list the results in Eq. (22),

$$\begin{cases} F|H \begin{cases} F_1|E = P_{\text{onehop}}(-(R-d), R), \\ F_1|!E = P_{\text{onehop}}(-0.5(R-d), R), \\ E|F_1 = P_{\text{hidden}}(R, 2R-d), \\ E|!F_1 = P_{\text{hidden}}(1.5R-0.5d, 2R-d), \end{cases} \\ F|!H \begin{cases} F_2|E = P_{\text{onehop}}(-(R-d), 0.5d), \\ F_2|!E = P_{\text{onehop}}(-0.5(R-d), 0.5d), \\ E|F_2 = P_{\text{hidden}}(R, 2R-d), \\ E|!F_2 = P_{\text{hidden}}(1.5R-0.5d, 2R-d), \end{cases} \\ H|F = P_{\text{hidden}}(R, R+d), \\ H|!F = P_{\text{hidden}}(R+0.5d, R+d) \end{cases} \tag{22}$$

3.4.2 One-hop collision probability

We derive the probabilities of one-hop collision in this part and analyze $F_1|E$ first. The two boundaries of F are $L_{\text{left}} = -R - d$ and $L_{\text{right}} = R$, respectively. Then, we can compute L_{center}, n_{car}, and n_{occupied} using Eqs. (17) – (20). The difference is that channel allocation in the one-hop collision area is a sampling process with replacement. Therefore, the one-hop collision probability is equal to

$$P_{\text{onehop}} = \left(\frac{n_{\text{slot}} - 1 - n_{\text{occupied}}}{n_{\text{slot}} - n_{\text{occupied}}}\right)^{n_{\text{car}}} \tag{23}$$

We denote Eq. (23) as $P_{\text{onehop}} = (L_{\text{left}}, L_{\text{right}})$. Similarly, $F_1|!E$, $F_2|E$, and $F_2|!E$ can also be derived using P_{onehop} by adjusting the boundary between the collision-free and one-hop area. We also list the results

in Eq. (22).

As discussed in Sections 3.4.1 and 3.4.2, all conditional probabilities can be derived by applying P_{hidden} and P_{onehop}. Figure 7 can be used to validate all the L_{left}s and L_{right}s in Eq. (22).

3.5 Probability of transmission interruption

As illustrated in Section 3.3, we express $P = 1 - p_{\text{rupt}}$ with a set of conditional probabilities. The classification and derivation of conditional probabilities are presented in Section 3.4. Eventually, the probability of transmission interruption p_{rupt} for different transmission distance d can be computed. We denote this function as $p_{\text{rupt}} = p_{\text{rupt}}(d; p_{\text{rr}}, R, \lambda)$ because p_{rr}, R, and λ will also affect p_{rupt}. The relationship between p_{rupt} and d under different conditions is illustrated in Fig. 8.

The increase in p_{rupt} with d is near linear. As mentioned in Section 2.1, p_{rupt} will be low when p_{rr} is low. This condition is desirable. If the average spacing between vehicles is 100 m, then the vehicle density for one lane will be 0. 01 vehicle/m. Thus, as illustrated in Fig. 8b, the total density for lanes 1, 2, 3, and 4 will be 0.01, 0.02, 0.03, and 0.04 vehicle/m, respectively. p_{rupt} is almost proportional to the number of lanes.

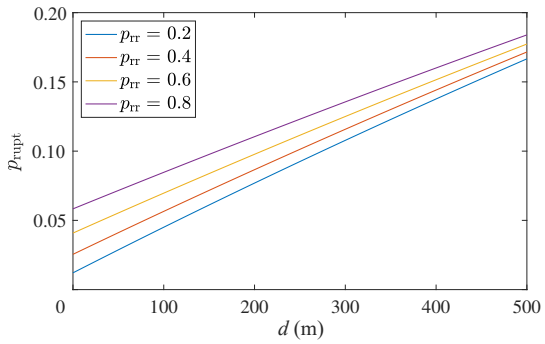

(a) $p_{\text{rupt}}(d; p_{\text{rr}} = 0.2, 0.4, 0.6, 0.8, R = 500\text{ m}, \lambda = 0.03\text{ vehicle/m})$

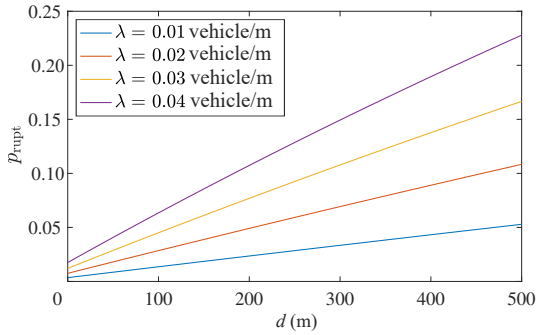

(b) $p_{\text{rupt}}(d; p_{\text{rr}} = 0.2, R = 500\text{ m}, \lambda = 0.01, 0.02, 0.03, 0.04\text{ vehicle/m})$

Fig. 8 Relationship between p_{rupt} and d.

3.6 Message transmission time

As discussed in the beginning of this section, the density function of transmission recovery time can be derived by using p_{rupt} (Section 3.5) and the density function of T_{rec} (Section 3.1). The probability of $\rho_{\text{lag}} \leqslant t$ is

$$f_{\rho_{\text{lag}}}(t; d, p_{\text{rr}}, R, \lambda) = 1 - p_{\text{rupt}}(d; p_{\text{rr}}, R, \lambda) \cdot (1 - f_{T_{\text{rec}}}(t)) \tag{24}$$

The graph of the cumulative density function $f_{\rho_{\text{lag}}}(t; d, p_{\text{rr}}, R, \lambda)$ based on Eq. (24) is displayed in Fig. 9.

4 Analysis of the RSS Strategy Supported by V2V Communication

As presented in this section, we evaluated the RSS strategy supported by V2V communication. We first illustrated the original RSS strategy[14] and the situation-aware RSS strategy[20] for car following. Then, we proposed an improved robust RSS strategy by considering the conditional distribution of the response time. Finally, we analyzed the system performance under two basic scenarios: vehicle platoon and approaching vehicle process.

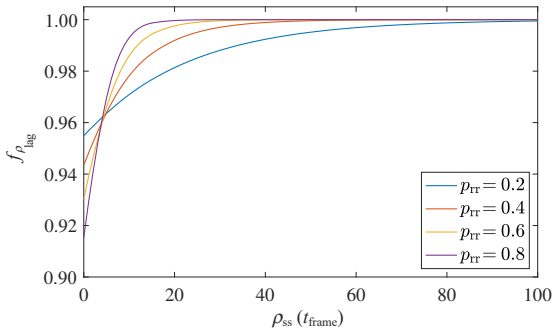

(a) $f_{\rho_{\text{lag}}}(t;\ d = 100\text{ m},\ p_{\text{rr}} = 0.2, 0.4, 0.6, 0.8,\ R = 500\text{ m},\ \lambda = 0.03\text{ vehicle/m})$

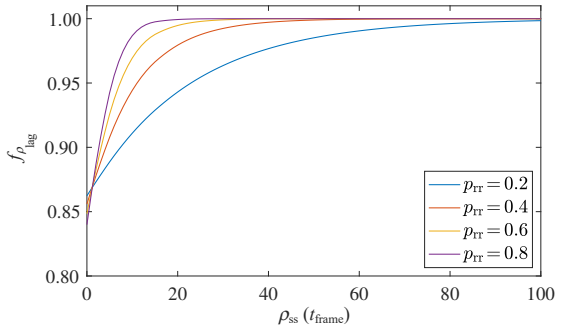

(b) $f_{\rho_{\text{lag}}}(t;\ d = 400\text{ m},\ p_{\text{rr}} = 0.2, 0.4, 0.6, 0.8,\ R = 500\text{ m}, \lambda = 0.03\text{ vehicle/m})$

Fig. 9 Cumulative density function of ρ_{lag}.

4.1 Original and situation-aware RSS strategy

The RSS model guarantees that the planning module will not erroneously assign autonomous vehicle responsibility[14]. The nomenclatures with regard to RSS strategy are given in Table 2 to illustrate the strategy.

When two consecutive vehicles move in the same lane in the same direction, the worst case scenario will be: (1) the leading vehicle brakes by at most $b_{\text{max, break}}$ until stopping fully, and (2) the following vehicle accelerates by at most $a_{\text{max, accel}}$ during the response time ρ and then brakes by at least $a_{\text{min, break}}$ after ρ until stopping fully. Then, the minimal safe longitudinal gap between vehicles should be the minimum distance that can ensure that collision does not occur in the worst case scenario. The result is

$$d_{\min}(t) = \Big[v_{\text{following}}\rho + \frac{a_{\text{max, accel}}\rho^2}{2} + \frac{(v_{\text{following}} + a_{\text{max, accel}}\rho)^2}{2a_{\text{min, brake}}} - \frac{v_{\text{leading}}^2}{2b_{\text{max, brake}}} \Big]_+ \tag{25}$$

The distance obtained by using Eq. (25) provides a sufficient condition for collision avoidance. However, parameters cannot achieve the boundary values simultaneously. Thus, this distance is unnecessarily large.

First, we can let the vehicle adopt large deceleration rates when braking if their speeds are large before braking[20],

$$a_{\text{brake}}(t) = a_{\text{min, brake}} + \frac{v_{\text{following}}}{v_{\max}}(a_{\text{max, brake}} - a_{\text{min, brake}}) \tag{26}$$

Table 2 Nomenclature list for the RSS strategy.

Symbol	Definition
$a_{\text{max, accel}}$	Maximum acceleration rate of the follower
$a_{\text{max, break}}$	Maximum deceleration rate of the follower
$a_{\text{min, break}}$	Minimum deceleration rate of the follower
$b_{\text{max, break}}$	Maximum deceleration rate of the leader
a_{accel}	General acceleration rate of the follower
a_{brake}	General deceleration rate of the follower
ρ	Response time
v_{leading}	Initial speed of the leader
$v_{\text{following}}$	Initial speed of the follower
$v_{\max}$	Maximum speed of vehicles
$d_{\min}$	Minimum gap between two vehicles
d	General gap between two vehicles
λ	Vehicle density
n_{lane}	Number of lanes
α_{safe}	Factor of safety

Furthermore, a highly efficient gap can be achieved by enabling vehicles to become aware of their situations[20]. The possible states of car-following are categorized into different types[20].

Following State: The following vehicle has already maintained a sufficiently close gap from the leading vehicle, and the speeds of the two vehicles are nearly identical in this situation. Thus, the following vehicle has absolutely no reason to accelerate during the response time.

$$d_{\min}^1(t) = \Big[v_{\text{following}}\rho + \frac{v_{\text{following}}^2}{2a_{\text{brake}}} - \frac{v_{\text{leading}}^2}{2b_{\text{max, brake}}} \Big]_+ \tag{27}$$

Approaching State: The following vehicle accelerates to catch up with the leading vehicle before it enters the following state. The safety distance can be calculated by letting the vehicle become aware of its acceleration.

$$d_{\min}^2(t) = \Big[v_{\text{following}}\rho + \frac{a_{\text{accel}}\rho^2}{2} + \frac{(v_{\text{following}} + a_{\text{accel}}\rho)^2}{2a_{\text{brake}}} - \frac{v_{\text{leading}}^2}{2b_{\text{max, brake}}} \Big]_+ \tag{28}$$

4.2 Improved robust RSS strategy

We continue to follow the assumption of situation awareness[20] introduced in Section 4.1. The setting of response time was improved. As discussed in Section 3, we found that: (1) ρ_{trans} is conditional on d, p_{rr}, λ, and R. In particular, the message transmission time is proportional to transmission distance d. (2) ρ_{trans} is a random variable, and we know the conditional probability distribution.

We want to minimize the gap between vehicles without affecting safety to increase traffic efficiency. The response time (message transmission time) decreases as the gap between vehicles decreases. Given this relationship, the required safety distance can be computed with a low response time. The rapid computation of the required safety distance indicates increased inefficiency. Distance between vehicles can be directly acquired in the vehicle communication system. Meanwhile, the number of vehicles in the radio range can be obtained. Thus, vehicle density can be computed. Therefore, in our improved RSS strategy, we allow the vehicle to adapt the response time with the change in d and λ.

Then, we discuss approaches for overcoming uncertainty. We can use the α_{safe}-percentile of ρ_{trans}, i.e., the value-at-risk of ρ_{trans} with a confidence level α_{safe}, by using a sufficiently large factor of safety

α_{safe} to guarantee that the following vehicle can brake without collision. Then, when an emergency occurs, we will have an α_{safe}-level confidence that the following vehicle can break in time to prevent collision. (α_{safe} is the probability of absolute safety. The probability of collision is less than $1-\alpha_{\text{safe}}$ because the RSS strategy is derived under the worst case scenario.)

To summarize, instead of setting a constant response time ρ, we set ρ on the basis of p_{rr} and R, and dynamically adjust it on the basis of d and λ. Given that $\rho_{\text{trans}} = t_{\text{pre}} + \rho_{\text{lag}} + t_{\text{react}}$, where t_{pre} and t_{react} can be set as constants, we have

$$\rho(d,\lambda;p_{\text{rr}},R) = t_{\text{pre}} + t_{\text{react}} + f_{\rho_{\text{lag}}}^{-1}(\alpha_{\text{safe}};d,p_{\text{rr}},R,\lambda) \tag{29}$$

We obtain the improved robust RSS by replacing the constant ρ in the situation-aware RSS with $\rho(d,\lambda;p_{\text{rr}},R)$ in Eq. (29).

The inverse function of $f_{\rho_{\text{lag}}}(t;d,p_{\text{rr}},R,\lambda)$ can be computed by using Eq. (24). Thus, $\rho(d,\lambda;p_{\text{rr}},R)$ can also be derived. The graph is displayed in Fig. 10. Small/large p_{rr} performs better for small/large d, respectively. However, the superiority of a large value of p_{rr} for a large value of d is more important than the superiority of a small value of p_{rr} for a small value of d. The trade-off between high and low p_{rr} is clarified.

4.3 Analysis of scenarios

4.3.1 Vehicle platoon scenario

As discussed in this section, we analyze a utopian scenario wherein all the vehicles on the highway (or 1–2 lanes of the highway) are equipped with LTE-V-Direct terminals. We consider this scenario because governments in some countries, including China, have increased their efforts to construct highways with LTE-V-Direct terminals.

In this scenario, all gaps between vehicles meet the minimum required safety distance and all vehicles

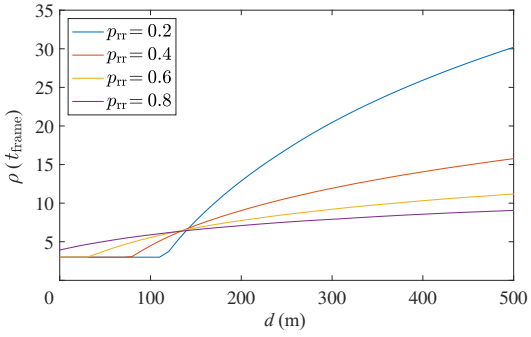

$\rho(d,\lambda=0.03\text{ vehicle/m};p_{\text{rr}}=0.2,0.4,0.6,0.8,R=500\text{ m})$

Fig. 10 Dynamic response time.

have identical speeds (Fig. 11). The required gaps of the original RSS and improved RSS can be derived directly by applying Eqs. (25) and (27), respectively. When we adopt LTE-V-Direct communication, the gap is determined by the response time. In turn, the response time is determined by the gap and vehicle density, whereas vehicle density is determined by the gap. Therefore, we must solve the following equations together to acquire the stationary conditions:

$$\begin{cases} d = \left[v_{\text{following}}\rho + \frac{v_{\text{following}}^2}{2a_{\text{brake}}} - \frac{v_{\text{leading}}^2}{2b_{\text{max, brake}}}\right]_+, \\ a_{\text{brake}} = a_{\text{min, brake}} + \frac{v_{\text{following}}}{v_{\max}}(a_{\text{max, brake}} - a_{\text{min, brake}}), \\ \rho = t_{\text{pre}} + t_{\text{react}} + f_{\rho_{\text{lag}}}^{-1}(\alpha_{\text{safe}};d,p_{\text{rr}},R,\lambda), \\ v_{\text{following}} = v_{\text{leading}}, \\ \lambda = \frac{n_{\text{lane}}}{d} \end{cases} \tag{30}$$

The first two equations follow the situation-aware RSS for the following state in Section 4.1. The third equation is the equation for the self-adapting response time proposed in Section 4.2. The fourth equation indicates that vehicles must maintain identical speeds, and the fifth equation is the relationship between density and spacing. Given any v_{leading}, we can solve the stationary conditions in Eq. (30) and obtain the stationary gaps.

In the numerical testing, we set $a_{\text{max, accel}} = 2\,\text{m}\cdot\text{s}^{-2}$, $a_{\text{max, brake}}=2.4\,\text{m}\cdot\text{s}^{-2}$, $a_{\text{min, brake}}=2\,\text{m}\cdot\text{s}^{-2}$, $b_{\text{max, break}}=2.4\,\text{m}\cdot\text{s}^{-2}$, and $v_{\max} = 45\,\text{m}\cdot\text{s}^{-1}$. The respond time of the original RSS strategy and improved RSS strategy is $\rho = 1.5\,\text{s}$. The parameters of LTE-V-Direct are set as $n_{\text{slot}} = 100$, $t_{\text{frame}} = 0.1\,\text{s}$, and $R = 200\,\text{m}$. We also set $\alpha_{\text{safe}} = 0.98$. Then the relationship between stationary spacing and speed is displayed in Fig. 12.

The improved robust RSS supported by LTE-V performs extremely well when $n_{\text{lane}} = 1$. Surprisingly, the stationary gap almost remains constant for different speeds. The gap between vehicles is easily controlled because it is indifferent to speed. Density is doubled when two lanes exist. Thus, the increased transmission lag increases the gap.

When vehicle density is high, a large p_{rr} is recommended to narrow the required distance. By contrast, when vehicle density is low, a small p_{rr} is recommended to improve efficiency. As discussed

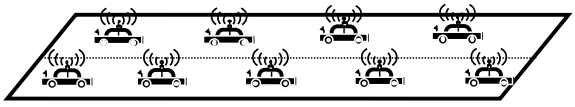

Fig. 11 Vehicle platoon scenario under the assumption of sufficiently high traffic flow.

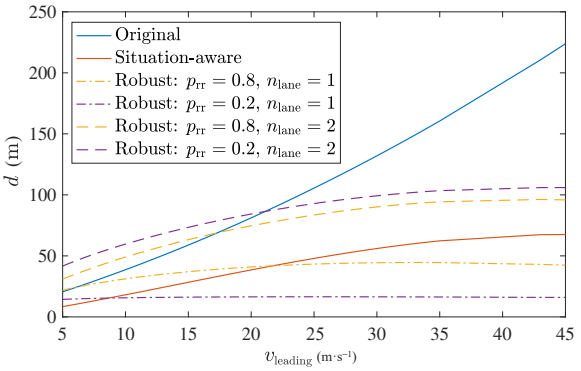

Fig. 12 Relationship between stationary gap and speed.

in Section 2, this is the trade-off when setting p_{rr}. Accordingly, no uniformly optimal MAC parameters exist under all conditions. We suggest that p_{rr} should be dynamically adjusted in accordance with real road situations.

4.3.2 Approaching vehicle scenario

Given that the first scenario is stationary, we now analyze a dynamic scenario: the approaching vehicle process. When the gap between two vehicles is considerably larger than the required safety distance, the following vehicle needs to accelerate to catch up with the leading vehicle (Fig. 13).

We use the following rules[20] to adjust the speed of the following vehicle for the original RSS, situation-aware RSS, and improved robust RSS. At time t, the vehicle first computes the required safety distance $d_{\min}$ in accordance with the strategy that the system adopts. Then, the vehicle compares the current distance with $d_{\min}$ and decides the speed at $t + t_{\text{frame}}$. If the current gap is larger than $d_{\min}$, we set

$$v_{\text{following}}(t + t_{\text{frame}}) = \min\{v_{\text{following}}(t) + a_{\text{max, accel}}\, t_{\text{frame}}, v_{\max}\} \quad (31)$$

If the current gap is smaller than $d_{\min}$, set

$$v_{\text{following}}(t + t_{\text{frame}}) = \max\{v_{\text{following}}(t) - a_{\text{min, break}}\, t_{\text{frame}}, v_{\text{leading}}\} \quad (32)$$

The vehicle must adjust its acceleration rate between the i-th frame to the $(i + 1)$-th frame to achieve this goal. Then, at time $t + t_{\text{frame}}$, the vehicle computes $d_{\min}$ again, and the above steps are reiterated.

In the numerical testing, we set $v_{\text{leading}} = 15\,\text{m}\cdot\text{s}^{-1}$.

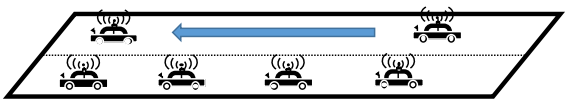

Fig. 13 Approaching vehicle scenario.

We also set $v_{\text{following}} = 15\,\text{m}\cdot\text{s}^{-1}$ and $d = 500\,\text{m}$ at the beginning $t = 0$. The parameters of LTE-V-Direct is set as $p_{rr} = 0.8$ and $R = 500\,\text{m}$. Other necessary parameters remain the same as those in the first scenario. Then we study the approaching process from $t = 0$ to when the gap reaches the minimum safety distance.

The trajectories of the leading vehicle and following vehicle using different strategies were derived in accordance with the above rules. The results are displayed in Fig. 14. The improved robust RSS is more efficient than other strategies because the response time of the original RSS and situation-aware RSS remain constant during approach, whereas that of the response time of the system based on LTE-V-Direct will decrease during approach.

5 Conclusion and Future Work

We provided an elaborate analysis of the latest LTE-V-Direct standards. We first modeled the MAC process of LTE-V-Direct on the basis of the Markov chain. Then, we applied the transmission recovery time and probability of transmission interruption as the bridges to derive the conditional probability distribution of transmission time. We found that when the resource reselection probability is low, the message transmission time remains extremely low for small transmission distance and then increases rapidly when distance exceeds the threshold value. By contrast, when resource reselection probability is high, transmission lag gradually increases with distance. This part can be regarded as an independent and comprehensive work on the LTE-V-Direct protocol. In addition to the use of models to analyze the collision avoidance system, this work can also be extended to the evaluation of the other functions of LTE-V-based systems.

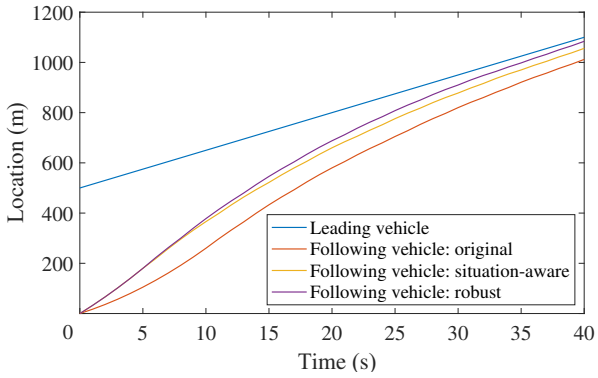

Fig. 14 Trajectory of vehicles during approach.

We also designed an improved robust RSS strategy based on the conditional probability distribution of transmission time. We found that the efficiency of RSS is further improved. This improvement not only relies on the low latency of V2V communication, but also on the fact that low transmission distances are associated with low lag. This relationship is a positive incentive for reducing gaps between vehicles. We analyzed the driverless highway scenario. Our analysis revealed that VAC vehicles supported by LTE-V-Direct can simultaneously maintain high speeds with stationary and narrow distances. This result illustrates the feasibility of setting a stationary required safety distance when only one lane exists. This approach will considerably simplify automated driving systems and proves that driverless highways can permit extremely high speed limits without affecting efficiency and safety if LTE-V is equipped. The above conclusions enhance the practicability of constructing driverless highways with one special lane reserved for the exclusive use of LTE-V vehicles. We also analyzed the dilemma of parameter setting. We conclude that parameter setting must be adjusted dynamically.

Although we adequately analyzed LTE-V in this work, we only considered oversimplified driving scenarios. Our control strategy is rudimentary and can only be utilized to describe uncomplicated driving scenarios. In the future, we will incorporate advanced control strategies with the LTE-V model to analyze highly complex scenarios.

Acknowledgment

This work was supported in part by the National Natural Science Foundation of China (No. 61673233), Beijing Municipal Science and Technology Program (No. D171100004917001/2), and the Key Technologies Research and Development Program of the Thirteenth Five-Year Plan of China (No. 2018YFB1600600).

References

[1] C. Diakaki, M. Papageorgiou, I. Papamichail, and I. Nikolos, Overview and analysis of vehicle automation and communication systems from a motorway traffic management perspective, *Transportation Research Part A: Policy and Practice*, vol. 75, pp. 147–165, 2015.

[2] L. Li and F.-Y. Wang, *Advanced Motion Control and Sensing for Intelligent Vehicles*. New York, NY, USA: Springer, 2007.

[3] S. Chen, J. Hu, Y. Shi, and L. Zhao, LTE-V: A TD-LTE-based V2X solution for future vehicular network. *IEEE Internet of Things Journal*, vol. 3, no. 6, pp. 997–1005, 2016.

[4] S. Chen, J. Hu, Y. Shi, Y. Peng, J. Fang, R. Zhao, and L. Zhao, Vehicle-to-everything (V2X) services supported by LTE-based systems and 5G, *IEEE Communications Standards Magazine*, vol. 1, no. 2, pp. 70–76, 2017.

[5] 3GPP, Evolved Universal Terrestrial Radio Access (E-UTRA) and Evolved Universal Terrestrial Radio Access Network (E-UTRAN); overall description; stage 2 (v14.3.0, Release 14), 3GPP Technical Report 36.300, 2017.

[6] 3GPP, Evolved Universal Terrestrial Radio Access (E-UTRA); physical layer procedures (v14.3.0, Release 14), 3GPP Technical Report 36.213, 2017.

[7] 3GPP, Evolved Universal Terrestrial Radio Access (E-UTRA); physical channels and modulation (v14.3.0, Release 14), 3GPP Technical Report 36.211, 2017.

[8] 3GPP, Evolved Universal Terrestrial Radio Access (E-UTRA); User Equipment (UE) radio transmission and reception (v14.4.0, Release 14), 3GPP Technical Report 36.101, 2017.

[9] 3GPP, Evolved Universal Terrestrial Radio Access (E-UTRA); Medium Access Control (MAC) protocol specification (v14.3.0, Release 14), 3GPP Technical Report 36.321, 2017.

[10] 3GPP, Evolved Universal Terrestrial Radio Access (E-UTRA); Radio Resource Control (RRC); protocol specification (v14.3.0, Release 14), 3GPP Technical Report 36.331, 2017.

[11] 3GPP, Architecture enhancements for V2X services (v14.3.0, Re- lease 14), 3GPP Technical Report 23.285, 2017.

[12] R. Molina-Masegosa and J. Gozalvez, LTE-V for sidelink 5G V2X vehicular communications: A new 5G technology for short-range vehicle-to-everything communications, *IEEE Vehicular Technology Magazine*, vol. 12, no. 4, pp. 30–39, 2017.

[13] X. Yang, J. Liu, F. Zhao, and N. H. Vaidya, A vehicle-to-vehicle communication protocol for cooperative collision warning, in *Proc. International Conference on Mobile & Ubiquitous Systems: Networking & Services*, Boston, MA, USA, 2004, pp. 22–25.

[14] S. Shalevshwartz, S. Shammah, and A. Shashua, On a formal model of safe and scalable self-driving cars, arXiv preprint arXiv: 1708.06374v5, 2018.

[15] N. Roohi, R. Kaur, J. Weimer, O. Sokolsky, and I. Lee, Self-driving vehicle verification towards a benchmark, arXiv preprint arXiv:1806.08810v1, 2018.

[16] M. Naumann, M. Lauer, and C. Stiller, Generating comfortable, safe and comprehensible trajectories for automated vehicles in mixed traffic, arXiv preprint arXiv: 1805.05374v1, 2018.

[17] R. Mariani, An overview of autonomous vehicles safety, in *Proc. 2018 IEEE International Reliability Physics Symposium (IRPS)*, Burlingame, CA, USA, 2018, doi: 10.1109/IRPS.2018.8353618.

[18] W. van Winsum and A. Heino, Choice of time-headway in car-following and the role of time-to-collision information in braking, *Ergonomics*, vol. 39, no. 4, pp. 579–592, 1996.

[19] X. Chen, L. Li, and Y. Zhang, A Markov model for headway/spacing distribution of road traffic, *IEEE Transactions on Intelligent Transportation Systems, vol.* 11, no. 4, pp. 773–785, 2010.

[20] L. Li, X. Peng, F. Wang, D. Cao, and L. Li, A situation-aware collision avoidance strategy for car-following, *IEEE/CAA Journal of Automatica Sinica*, vol. 5, no. 5, pp. 1012–1016, 2018.

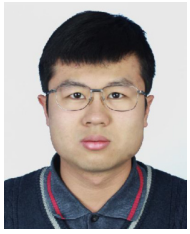

Jiayang Li is currently an undergraduate student at Tsinghua University with his major research interests including intelligent vehicle-infrastructure cooperative systems, traffic data analysis, and traffic system management.

Yi Zhang received the BS degree in 1986 and the MS degree in 1988 from Tsinghua University in China, and earned the PhD degree in 1995 from the University of Strathclyde in UK. He is a professor in control science and engineering at Tsinghua University with his current research interests focusing on intelligent transportation systems. His active research areas include intelligent vehicle-infrastructure cooperative systems, analysis of urban transportation systems, urban road network management, traffic data fusion and dissemination, and urban traffic control and management. His research fields also cover the advanced control theory and applications, advanced detection and measurement, systems engineering, etc.

Mengkai Shi received the BEng degree in 2013 and the PhD degree in 2018 from Tsinghua University, China. He is an engineer at Beijing Nebula Link Technology Co., Ltd. He has participated several research projects granted from MOST, NSFC, and some companies. His research interests include intelligent transportation system, intelligent vehicle infrastructure cooperation systems, VANET, connected vehicles, and cooperative driving.

Qi Liu received the BS degree in 1999 and PhD degree in 2003 from Beijing Jiaotong University, respectively. She is a professor of engineering and the director of IoV in China Unicom Network Technology Research Institute. Her main research fields include IoV, 5G, networks convergence, and high accuracy positioning. More than 30 high-level papers have been published in academic journals both at home and abroad, 2 scholarly monographs have been published. And more than 40 patents of invention have been applied. She has undertaken several national major research projects, and has won provincial and ministerial awards, including the science and technology award of China Communications Society, She participated in multiple of major academic exchanges at home and abroad, and delivered speeches.

Yi Chen received the bachelor degree from Tianjin University in 2012 and the master degree from Beijing University of Posts and Telecommunications in 2015. Her major is telecommunication engineering. She has worked in China Unicom as a telecommunication engineer from 2015 until now. Her interests include wireless communication technology, C-V2X technology, and high-precision positioning technology. She has published 1 book as the co-author, and more than 4 papers in related areas. The projects she participated in have received the provincial and ministerial award and China Unicom science and technology progress award.